

This discussion paper is/has been under review for the journal Biogeosciences (BG).  
Please refer to the corresponding final paper in BG if available.

# Extreme events in gross primary production: a characterization across continents

J. Zscheischler<sup>1,2,3</sup>, M. D. Mahecha<sup>1</sup>, S. Harmeling<sup>2</sup>, A. Rammig<sup>4</sup>, E. Tomelleri<sup>1,\*</sup>,  
and M. Reichstein<sup>1</sup>

<sup>1</sup>Max Planck Institute for Biogeochemistry, Jena, Germany

<sup>2</sup>Max Planck Institute for Intelligent Systems, Tübingen, Germany

<sup>3</sup>Institute for Atmospheric and Climate Science, ETH Zürich, Switzerland

<sup>4</sup>Potsdam Institute for Climate Impact Research, Potsdam, Germany

\* now at: EURAC, Institute for Applied Remote Sensing, Bozen, Italy

Received: 19 December 2013 – Accepted: 22 January 2014 – Published: 31 January 2014

Correspondence to: J. Zscheischler (jzsch@bgc-jena.mpg.de)

Published by Copernicus Publications on behalf of the European Geosciences Union.

BGD

11, 1869–1907, 2014

GPP extremes across continents

J. Zscheischler et al.

Title Page

Abstract

Introduction

Conclusions

References

Tables

Figures

◀

▶

◀

▶

Back

Close

Full Screen / Esc

Printer-friendly Version

Interactive Discussion



## Abstract

Climate extremes can affect the functioning of terrestrial ecosystems, for instance via a reduction of the photosynthetic capacity or alterations of respiratory processes. Yet the dominant regional and seasonal effects of hydrometeorological extremes are still not well documented. Here we quantify and characterize the role of large spatiotemporal extreme events in gross primary production (GPP) as triggers of continental anomalies. We also investigate seasonal dynamics of extreme impacts on continental GPP anomalies. We find that the 50 largest positive (increase in uptake) and negative extremes (decrease in uptake) on each continent can explain most of the continental variation in GPP, which is in line with previous results obtained at the global scale. We show that negative extremes are larger than positive ones and demonstrate that this asymmetry is particularly strong in South America and Europe. Most extremes in GPP start in early summer. Our analysis indicates that the overall impacts and the spatial extents of GPP extremes are power law distributed with exponents that vary little across continents. Moreover, we show that on all continents and for all data sets the spatial extents play a more important role than durations or maximal GPP anomaly when it comes to the overall impact of GPP extremes. An analysis of possible causes implies that across continents most extremes in GPP can best be explained by water scarcity rather than by extreme temperatures. However, for Europe, South America and Oceania we identify also fire as an important driver. Our findings are consistent with remote sensing products. An independent validation against a literature survey on specific extreme events supports our results to a large extent.

## 1 Introduction

The terrestrial carbon cycle is tightly linked to the global climate system. Favorable conditions for vegetation in the future are expected to increase terrestrial carbon uptake, while extreme climatic conditions might drastically decrease this uptake (Reichstein

**BGD**

11, 1869–1907, 2014

## GPP extremes across continents

J. Zscheischler et al.

Title Page

Abstract

Introduction

Conclusions

References

Tables

Figures

◀

▶

◀

▶

Back

Close

Full Screen / Esc

Printer-friendly Version

Interactive Discussion



et al., 2013). Separating the enhancing and attenuating effects of growth in the terrestrial biosphere requires, besides others, a precise understanding of the feedbacks between climate extremes and terrestrial carbon fluxes.

The impacts of climate extremes on ecosystems and the carbon cycle are diverse. Storms transform carbon stocks from living biomass to dead wood and thus increase the risk of fire and pathogen outbreaks (Negrón-Juárez and Chambers, 2010). Droughts and heat waves have an impact on plant physiology, phenology and carbon allocation (Ciais et al., 2005; Reichstein et al., 2007; Phillips et al., 2009). Inevitable consequences are often increased tree mortality, higher fire risks and susceptibility to pathogens. On the long term, droughts might also influence vegetation composition. Due to lagged effects like increased tree mortality in years after a severe drought (Bréda et al., 2006; Bigler et al., 2007) or changes in the respiration of soil heterotrophic organisms a year after an anomalously warm season (Arnone et al., 2008), impacts of droughts on the carbon cycle are difficult to assess generally. Fires have an immediate and large impact on carbon stocks and vegetation structure (Westerling et al., 2006; Field et al., 2009). Ice storms and frost may cause physical damage up to whole-stand destruction (Irland, 2000; Sun et al., 2012). Hence, it is a major challenge to design an analytic approach that consistently quantifies the diverse impacts of climate extremes on the terrestrial biosphere.

Past studies often first identified extreme events in climate variables or other drivers and subsequently analyzed their aftermath in ecosystems and the carbon cycle (Page et al., 2002; Ciais et al., 2005; Kurz et al., 2008; Zeng et al., 2009; Zhao and Running, 2010). This forward approach is appealing because one can, for instance, focus on a certain region or specific time span and concentrate on one extreme event with all its consequences. However, such an event-based analysis can easily lead to a biased perception of extreme events. Extreme events that affect regions of social or economic interest gain more attention than extreme events in regions with less public interest. For instance, very few experimental studies are done in Africa. Furthermore, climate extremes do not necessarily lead to extreme responses of the biosphere. Inversely,

**BGD**

11, 1869–1907, 2014

## GPP extremes across continents

J. Zscheischler et al.

Title Page

Abstract

Introduction

Conclusions

References

Tables

Figures

◀

▶

◀

▶

Back

Close

Full Screen / Esc

Printer-friendly Version

Interactive Discussion



## GPP extremes across continents

J. Zscheischler et al.

Title Page

Abstract

Introduction

Conclusions

References

Tables

Figures

◀

▶

◀

▶

Back

Close

Full Screen / Esc

Printer-friendly Version

Interactive Discussion



not all extreme responses of the terrestrial biosphere are unambiguously explicable by some climate extreme or disturbance event. For instance, a very unlikely constellation of drivers with each of them being not extreme in its own domain might still cause extreme changes in ecosystems (so-called *compound extremes*, IPCC, 2012; Leonard et al., 2013). To tackle some of these drawbacks, Smith (2011) suggested the definition of *extreme climatic event* (ECE) as “an episode or occurrence in which a statistically rare or unusual climatic period alters ecosystem structure and/or function”. A pure forward analysis, instead, is always at the risk of overlooking extreme changes in the state of the biosphere and hence not desirable.

In a recent study, Zscheischler et al. (2014) presented a quantification of negative extremes in of Gross Primary Production (GPP) based on four different data sets at global scale. This study explicitly adopted an impact driven perspective (Reichstein et al., 2013), aiming for an assessment of globally relevant extreme changes in an impact variable. By an impact variable we understand a variable describing the state of the biosphere including the fraction of absorbed photosynthetically active radiation (fAPAR), leaf area index (LAI), the enhanced vegetation index (EVI), or biosphere–atmosphere carbon exchange.

A classical approach to identify extremes in time series is based on Extreme Value Theory (EVT, Coles, 2001; Ghil et al., 2011). Samples exceeding a specific threshold are modeled using certain extreme value distributions. This approach is called Peak Over Threshold method (POT). Gumbel (2004) showed that for any well behaved initial distribution only a few models are needed. However, because the sample size is limited by the samples exceeding the set threshold, this approach is not feasible in our case where we are confronted with relatively short time series. Moreover, we are interested in those extremes that affect larg contiguous areas and/or long time periods. More formally, we are interested in the “volume of extreme events” which we understand as three-dimensional structures contiguous in time and space where each single value exceeds a certain threshold. For that reason, here we use an alternative approach mo-

tivated by a three-dimensional drought assessment (Lloyd-Hughes, 2012; Zscheischler et al., 2013).

In this contribution, we directly follow up on Zscheischler et al. (2014) where it could be shown that a few extreme events in GPP explain most of its interannual variability and investigate the underlying regional patterns and temporal dynamics. In particular, we will look for regions in time and space where carbon uptake is much lower compared to normal conditions. We will then trace these extreme changes back to anomalous meteorological variables or fires and aim at understanding continental differences. It has been suggested earlier that the size distribution of extreme events in the biosphere follow a power law (Zscheischler et al., 2013, 2014; Reichstein et al., 2013). Here we investigate whether this power law behavior is robust across continents and different spatial and temporal resolutions. To validate our approach we compare the spatial patterns of GPP extreme events with extremes in independent remote sensing products and the current literature.

## 2 Material and methods

### 2.1 Data

To identify extreme events that are relevant for the terrestrial carbon exchange and hence the terrestrial biosphere, we rely on four different data sets describing Gross Primary Production (GPP) which cover the last 30 yr (1982–2011). The range of the data sets spans from purely data driven (upscaled model tree ensemble, (*MTE*, Jung et al., 2011)) over semi-empirical (based on light-use efficiency, *MOD17+*, Running et al., 2004) towards process-based global ecosystem (Lund–Potsdam–Jena Dynamic Global Vegetation Model for managed Land, *LPJmL*, Sitch et al., 2003) and land-surface models (*OCN*, Zaehle and Friend, 2010).

*MTE* involves training a Model Tree Ensemble at site level using FLUXNET (a global network of eddy covariance observations in tandem with site level meteorology, Bal-

**BGD**

11, 1869–1907, 2014

## GPP extremes across continents

J. Zscheischler et al.

Title Page

Abstract

Introduction

Conclusions

References

Tables

Figures

◀

▶

◀

▶

Back

Close

Full Screen / Esc

Printer-friendly Version

Interactive Discussion



docchi et al., 2001) to extrapolate to large spatiotemporal domains. We use a fully data driven upscaling product that relies mainly on a composite of different remote sensing fAPAR products but also uses climate data from ERA interim (Dee et al., 2011).

*MOD17+* is derived using the same model structure as the MODIS GPP data stream (Running et al., 2000) linking shortwave incoming radiation, minimum temperature and vapor pressure deficit. The model parameterization of Beer et al. (2010), based on Bayesian inversion against GPP time series from FLUXNET, is applied here. The terms in the MODIS-MOD17 biome-specific look-up table are used as priors. For regionalizing the model parameters we stratify the results of the in-situ calibration per vegetation type and bioclimatic class. As climatic drivers we use the ERA-interim dataset and the same composite of fAPAR products as in MTE (Jung et al., 2011).

*LPJmL* is a dynamic vegetation model that mechanistically represents plant physiological and biogeochemical processes (Sitch et al., 2003) including the hydrological cycle (Gerten et al., 2004) and a process-based fire model (Thonicke et al., 2010). Vegetation is in the model represented as plant functional types (PFTs), which are described by their bioclimatic limits, and morphological, phenological and physiological parameters. The model is also capable to simulate agricultural land (crop functional types, Bondeau et al., 2007) but for the present study, the model is applied in its natural vegetation mode. For each PFT, the model simulates photosynthesis (based on Farquhar et al. (1980) with adjustment of carboxylation capacity and leaf nitrogen seasonally and within the canopy profile (Haxeltine and Prentice, 1996)) and respiration, and the allocation of accumulated carbon to the plant's compartments (leaves, stem, root and reproductive organs).

*OCN* is a land-surface model derived from the ORCHIDEE DGVM (Krinner et al., 2005), which prognostically simulates foliar area and N content and employs a two-stream radiation scheme coupled to the process-based calculation of photosynthesis in light-limited and light-saturated chloroplasts within each canopy layer (Friend and Kiang, 2005).

**BGD**

11, 1869–1907, 2014

## GPP extremes across continents

J. Zscheischler et al.

Title Page

Abstract

Introduction

Conclusions

References

Tables

Figures

◀

▶

◀

▶

Back

Close

Full Screen / Esc

Printer-friendly Version

Interactive Discussion



AVG is the average of the above four data sets. Although in most cases we will report averaged results of MTE, MOD17+, LPJmL and OCN, we will also compute extremes on the averaged data set assuming that averaging levels out artifacts of individual data sets and emphasizes common features.

To attribute GPP extreme events to climatic drivers we use temperature ( $T$ ) and precipitation ( $P$ ) from bias corrected ERA-interim (Dee et al., 2011) as used by the models predicting GPP, the water availability index (WAI), burned area (BA), and CO<sub>2</sub> emissions from fires (FE, Giglio et al., 2010). WAI is a surrogate for soil moisture and was computed according to Prentice et al. (1993) using daily precipitation and potential evapotranspiration data from ERA Interim and a map of plant available water holding capacity from the Global Harmonized World Soil Database. The spatial resolution for all above data sets is 0.5°.  $T$ ,  $P$ , WAI and all GPP data sets are available monthly from 1982–2011, BA and FE from 1997–2010.

To compare results obtained from the GPP data sets (in particular hot spots of extreme events and scaling behavior) with other remote sensing products we use the following data sets. A composite of the fraction of absorbed photosynthetically active radiation (fAPAR, Jung et al., 2011) and the leaf area index (LAI, Liu et al., 2012) from 1982–2011 on a 0.5° spatial and monthly temporal resolution, the enhanced vegetation index from MODIS (EVI, Huete et al., 2002) from 2001–2011 on a 0.5° spatial and 8 day temporal resolution, and GPP from MODIS (MODISGPP, Running et al., 2004) from 2001–2011 on a 0.1° spatial and 8 day spatial resolution.

We define six areas for the continental cutouts from the 26 areas of the SREX report of the IPCC (2012) (Fig. 2 in Zscheischler et al., 2013). The areas are aggregated as follows: North America 1–6, South America 7–10, Europe 11–13, Africa 14–17, Asia 18–23, Oceania 24–26.

## 2.2 Preprocessing

For  $T$ , WAI, EVI, fAPAR, LAI, and all GPP data sets we first subtract linear trend and then the mean annual cycle at each pixel to obtain anomalies comparable across time.

## GPP extremes across continents

J. Zscheischler et al.

Title Page

Abstract

Introduction

Conclusions

References

Tables

Figures

◀

▶

◀

▶

Back

Close

Full Screen / Esc

Printer-friendly Version

Interactive Discussion



## 2.3 Extreme event identification

In accordance with the IPCC climate extreme classifications (Seneviratne et al., 2012), we define *extremes* as the occurrence of certain values in the tails of the probability distribution of the anomalies. We define extremes to be outside a certain threshold  $q$  which is defined by a percentile on the absolute values of the anomalies (Fig. 1). We choose the thresholds for each of the four data sets such that extremes (positive and negative together) comprise 1, . . . , 10% of the anomalies at each continent separately. We then define an *extreme event* by spatiotemporally contiguous values being larger than  $q$  (positive extremes) and smaller than  $-q$  (negative extremes), respectively. To decide whether two elements in a 3-D data cube, so-called *voxels* (short for volumetric pixel, used e.g. in Neuroscience or computer gaming), are connected, different definitions are possible. Naturally, for a three-dimensional data set, connectivities of 6, 18 and 26 are possible. A connectivity of 6 means, that only horizontal or vertical neighbors are considered as connected to it (each voxel has 6 horizontal and vertical neighbors). A connectivity of 18 means that all neighbors in the  $3 \times 3 \times 3$  neighborhood of one voxel count as connected, excluding the 8 corners ( $3 \times 3 \times 3 = 27 - 8 \text{ corners} - \text{center} = 18$ ), while a connectivity 26 means that all 26 vertical, horizontal and diagonal neighbors are considered as connected to the central voxel ( $27 - 1 = 26$ ). Note that in principle, the connectivity could also extend over more than one neighboring pixel (Lloyd-Hughes, 2012). Throughout most of this study, we will use a connectivity of 26. We generally compute the largest 200 positive and negative GPP extreme events on each continent.

To evaluate the sensitivity of our method to some of the relevant parameters, we will analyze the scaling behavior of different temporal and spatial resolutions as well as different definitions of connectivity on the MODISGPP data set, which is available in high temporal and spatial resolution. To evaluate spatial patterns of hot spots we compare our results with the same extreme event detection approach on EVI, fAPAR, LAI and the mean of the four  $0.5^\circ$  GPP data sets.

BGD

11, 1869–1907, 2014

### GPP extremes across continents

J. Zscheischler et al.

Title Page

Abstract

Introduction

Conclusions

References

Tables

Figures

◀

▶

◀

▶

Back

Close

Full Screen / Esc

Printer-friendly Version

Interactive Discussion



## 2.4 Nomenclature

The integral of anomalies over time and space comprising one GPP extreme event is called *overall impact* of an event. Its *spatial extent* is the maximal spatial extent of all pixels contained in the event, independent from the time. *Duration* is the maximal length of an event in months. An event computed using 5th-percentiles is called a *5th-percentile extreme*.

## 2.5 Statistics on extreme events

We test whether the distributions of overall impacts and spatial extents of extreme events follow power laws following the suggestions by Clauset et al. (2009). We assess whether positive and negative extreme events are equally big by dividing the  $n$  largest negative events by the  $n$  largest positive events. To study asymmetry at pixel scale we subtract global maps of negative and positive extremes from each other (see below).

The impact of extreme events can be analyzed in time or space. For a temporal analysis, all anomalies in any extreme event (according to the definition under consideration) are summed over a time step in the region of interest. This summation yields one regional time series of the total impact of the respective extreme events. Such time series of GPP extremes can then be correlated with e.g. the continental GPP anomaly in order to obtain the fraction of explained variance. Similarly, for an analysis in space, all anomalies during extreme events are summed together at a specific location (pixel). A summation of this type leads to a map of the cumulative impact of the extreme events under consideration.

We compute the number of extreme events starting at each month in the year to analyze whether there is a seasonality in the occurrence of GPP extreme events. To assess which factors are most responsible for the overall impact of a GPP extreme event we correlate the overall impact of events against spatial extent, duration and maximal anomaly of the event. To investigate the influence of the resolution and connectivity on the power law coefficient we perform a 3-way ANOVA with the factors spatial resolution

BGD

11, 1869–1907, 2014

## GPP extremes across continents

J. Zscheischler et al.

Title Page

Abstract

Introduction

Conclusions

References

Tables

Figures

◀

▶

◀

▶

Back

Close

Full Screen / Esc

Printer-friendly Version

Interactive Discussion



(0.1°, 0.5°, 1°), temporal resolution (8 days, 16 days, monthly) and connectivity (6, 18, 26).

## 2.6 Attributing drivers to GPP extremes

We follow Zscheischler et al. (2013) to identify drivers that possibly caused extremes in GPP on each continent separately. More specifically, for a certain GPP extreme event we compute the median of a driver variable over the same region. By shifting the event in time and computing such medians for each possible time shift, we obtain a test statistic for each driver variable and each GPP extreme event. We then compute  $p$  values for the 200 largest negative 1st-percentile events of each GPP data set on each continent where we use the drivers  $T$ ,  $P$ , WAI, BA, FE and count a driver as “cause” if  $p < 0.1$ . Accordingly, if a driver and GPP are not related one would expect on average 10% of the events “caused” by that driver. The choice of the threshold is arbitrary and reflects how conservative the researcher wants to be. Our general conclusions are not sensitive to the specific choice of this parameter.

## 2.7 Literature validation

The mere number of extreme events makes it difficult to compare the data sets event by event. In this study we focus on the largest event of each data set per continent. In order to evaluate our detection approach against some independent evidence, we perform a literature search where we searched for hints that the largest negative GPP extreme events (5 data sets  $\times$  6 continents = 30 in total) are reported in case studies. We compare this to well-known extremes in climate but also other variables in the literature that might have reduced the carbon uptake substantially.

**BGD**

11, 1869–1907, 2014

## GPP extremes across continents

J. Zscheischler et al.

Title Page

Abstract

Introduction

Conclusions

References

Tables

Figures

◀

▶

◀

▶

Back

Close

Full Screen / Esc

Printer-friendly Version

Interactive Discussion



### 3 Results and discussion

#### 3.1 Extreme events in GPP are power law distributed

Power laws have been studied in a variety of applications. In ecology, most often they occur either as bivariate relationships, e.g. population density–body mass (Marquet et al., 1990) or frequency size distributions, e.g. body sizes (Morse et al., 1985), vegetation patches (Kéfi et al., 2007) fire magnitudes (Turcotte et al., 2002) or canopy gaps (Asner et al., 2013). Mathematically, a variable is following a power law if it is drawn from a probability distribution

$$p(x) \propto x^{-\alpha}, \quad (1)$$

where  $\alpha$  is the *scaling parameter*. Earlier attempts to describe disturbance events in form of power laws were restricted to their spatial extent (Fisher et al., 2008; Gloor et al., 2009; Kellner and Asner, 2009; Asner et al., 2013). It has recently been shown that also the overall impacts of negative extreme events in fAPAR (Zscheischler et al., 2013) and GPP (Zscheischler et al., 2014) can be well approximated by power laws at the global scale. Here, we look at each continent separately and also consider the spatial extent of extreme events.

Overall, the exponents  $\alpha$  of the overall impacts of an event are lower than the exponents of the spatial extents (1.69 vs. 1.86 on average, Fig. 2). We also notice a slight upward trend for more extreme percentiles. Except for a few values most of the exponents of GPP extremes defined by the 5th percentile or higher are well in the range between 1.55–1.75, and 1.65–1.95 for overall impact and spatial extent, respectively. Hence, the values for the spatial extent fall in the range of exponents recently estimated for canopy gaps in tropical forests ( $\alpha = 1.83 \pm 0.09$ , Asner et al., 2013). Such low power law exponents ( $\alpha < 2.0$ ) imply that the distribution of extremes is largely dominated by few very large events, as has been discussed for the case of canopy gaps (Fisher et al., 2008; Asner et al., 2013).

BGD

11, 1869–1907, 2014

## GPP extremes across continents

J. Zscheischler et al.

Title Page

Abstract

Introduction

Conclusions

References

Tables

Figures

◀

▶

◀

▶

Back

Close

Full Screen / Esc

Printer-friendly Version

Interactive Discussion



## GPP extremes across continents

J. Zscheischler et al.

Title Page

Abstract

Introduction

Conclusions

References

Tables

Figures

◀

▶

◀

▶

Back

Close

Full Screen / Esc

Printer-friendly Version

Interactive Discussion



Power laws can have a variety of origins (Newman, 2005; Sornette, 2006). In case of spatiotemporal extreme events a couple of explanations are possible. Because we set a threshold to obtain extreme events, thresholding of stochastic processes (Touboul and Destexhe, 2010) or the theory of large deviation (Varadhan, 1966; Sornette, 2006) might provide reasonable explanations. In ecology it has been shown that power laws can emerge from a complex interplay of spatial interactions (Pascual and Guichard, 2005; Pueyo et al., 2010). Additionally, for multidimensional lattices, even without any spatial interaction, it follows from percolation theory (Bollobas and Riordan, 2006) that the size distribution of random clusters can follow a power law. Whether the emergent power laws for overall impact and spatial extent arise from a combination of the above mentioned mechanisms, or whether there is an even different mechanism generating these, cannot be conclusively resolved here and needs further investigation.

As already stated above, in variables that are power law distributed, very few elements can dominate the whole distribution (depending on the power law exponent  $\alpha$ ). To understand the importance of individual extreme events, we investigate how much of each continents variability in GPP can be explained by extremes in GPP. It has been shown recently that at global scale about 200 extreme events can explain nearly 80 % of the global anomaly (Zscheischler et al., 2014). On the continental level, 50 positive and negative events are enough to obtain an averaged correlation coefficient with continental anomaly between 0.88 (Asia) and 0.95 (Oceania) (Fig. 3).

For 1st-percentile extremes the spatial extent is the dominating factor (as already mentioned in Reichstein et al., 2013), while the duration and maximal anomaly play a minor role. This relation changes only little throughout the continents (Fig. 4). For 10th-percentile extremes the duration gains on importance and has similarly high correlations with overall impact as the spatial extent (not shown).

### 3.2 Global distribution of GPP extremes

The averaged map of an average year of the 200 largest negative 10th-percentile GPP extreme events computed for each continent is visually nearly identical with the av-

eraged map for the globally largest 1000 extreme events (Fig. 5, cf. Figure 3a in Zscheischler et al., 2014). We find that mostly savannas and grasslands are hit by large-scale extremes in GPP. The regions which experience the largest GPP extreme events on average at global scale include Caatinga (Brazil), the Pantanal (Brazil), the Great Plains (US), the grasslands connecting Kenya, Tanzania and Uganda (Africa), Highveld (South Africa), the Indus–Ganga Plain (India), and Eastern Australia.

At a continental perspective extremes in GPP are largest in Asia (on average  $0.87 \text{ PgCyr}^{-1}$  for 10th-percentile extremes, ranging from  $0.50 \text{ PgCyr}^{-1}$  in MOD17+ to  $1.35 \text{ PgCyr}^{-1}$  in LPJmL) and lowest in Europe (on average  $0.23 \text{ PgCyr}^{-1}$  for 10th-percentile extremes, ranging from  $0.13 \text{ PgCyr}^{-1}$  in MTE to  $0.41 \text{ PgCyr}^{-1}$  in LPJmL, Fig. 6a–f). The overall impact of extreme events in GPP obviously depends on the size of the continent. The spread between the data sets is similar for each continent. However, in all continents the two models (LPJmL and OCN) exceed the two data driven approaches (MTE and MOD17+) by a factor of at least two. Studies that compare model and data-driven GPP products found that the interannual variability of GPP is generally lower in MTE compared to carbon cycle models (Jung et al., 2011; Keenan et al., 2012; Piao et al., 2013). In South America, the two models agree very well, while in Europe and Africa the two data driven approaches nearly coincide (Fig. 6b–d). The magnitude of extremes in the averaged data set AVG lies at the lower range of the four other data sets. The averaging process levels out the tails of the distributions of the anomalies of the individual data sets (where those do not agree among each other) and hence contains less strongly pronounced extremes as can also be seen from a histogram of the anomalies (not shown). The difference between the averaged extremes and the extremes of the averaged data set (Fig. 7) highlights again that extremes in AVG are generally smaller. Yet in tropical areas, in particular in densely vegetated regions, the extremes in AVG exceed the averaged extremes of the individual four data sets. This suggests that the data sets agree rather well in densely vegetated regions albeit the lower magnitude of extremes.

## BGD

11, 1869–1907, 2014

### GPP extremes across continents

J. Zscheischler et al.

Title Page

Abstract

Introduction

Conclusions

References

Tables

Figures

◀

▶

◀

▶

Back

Close

Full Screen / Esc

Printer-friendly Version

Interactive Discussion



Negative GPP extreme events mainly start in summer, both in the northern and Southern Hemisphere except Oceania (Fig. 8). This pattern is much stronger pronounced in the northern continents, presumably because of less pronounced seasonal differences in the tropical regions and the more land area in northern latitudes than in southern latitudes. For South America and Africa the increasing number of extremes coincides with the end of the dry season and with the wet season (ONDJ).

### 3.3 Positive extremes offset negative extremes only partly

It has been shown recently that, on a global scale, negative extreme events in GPP are larger than positive extremes (Zscheischler et al., 2014). One question we want to address here is if this observations holds for all continents. The observed global asymmetry seems to be mainly generated by asymmetries in South America and Europe (Fig. 6h and i). In Africa and Asia, instead, positive and negative GPP extremes are balanced, whereas in Oceania the positive extremes are slightly larger (Fig. 6j–l). The averaged data set *AVG*, in contrast, exhibits a strong asymmetry towards larger negative GPP extreme events for all continents except Asia (Fig. 6h–l).

Figure 9 shows an average of the pixel-wise difference between the largest 200 positive and negative 10th-percentile GPP extreme events in MTE, MODSI17+, LPJmL and OCN (a), and the pixel-wise difference between the largest 200 positive and negative 10th-percentile GPP extreme events of *AVG* (b), respectively. The patterns are similar in most regions of the world. The asymmetry between negative and positive extremes in GPP hence seems to be a robust feature, which persists through the averaging process. Although it seems that overall the regions with larger negative extremes do not dominate at global scale (Fig. 9, blue and red occupy a similar amount of land surface), their magnitude is often much larger. Also, in most tropical regions negative extremes are dominating (blue dominates in tropical areas).

**BGD**

11, 1869–1907, 2014

## GPP extremes across continents

J. Zscheischler et al.

Title Page

Abstract

Introduction

Conclusions

References

Tables

Figures

◀

▶

◀

▶

Back

Close

Full Screen / Esc

Printer-friendly Version

Interactive Discussion



### 3.4 Influence of resolution and connectivity on the scaling parameter

One may remark that the identified scaling behavior (the exponents of the power law) of the GPP extremes is partly an effect of spatial resolution and chosen connectivity (cf. Sect. 3.1). In order to investigate this issue, we use MODISGPP to analyze the sensitivity of the power law exponent to the spatial and temporal resolution because MODISGPP is available on higher resolutions than the four data sets we have analyzed before. We can detect a dependence of  $\alpha$  to the spatial and temporal resolution as well as to the connectivity (3-way ANOVA,  $p < 0.05$  in 81 % and 69 % of the cases for overall impact and spatial extent, respectively), but the effects are remarkably small. The mean over the exponent  $\alpha$  for the distribution of overall impacts for all continents and all configurations is  $1.87 \pm 0.09$ . For the spatial extent we obtain a mean of  $1.97 \pm 0.14$ . This suggests that the emergent power law behavior in size and spatial extent is a robust feature of extreme events in GPP.

### 3.5 Water scarcity as the dominant driver for negative extreme events

Recent studies identified water scarcity as the globally dominant driver for negative extreme GPP events (Reichstein et al., 2013; Zscheischler et al., 2014). Breaking down the analysis to the continental level supports these findings in general. The patterns for the different data sets look alike (Fig. 10) although differing slightly in magnitude. GPP in LPJmL is most sensitive to droughts (on average 76 % of the GPP extremes could be associated with low levels of WAI, Fig. 10, orange bars). But there are also some differences between continents. In Europe, GPP does not seem to be as susceptible to droughts as in the other continents. Here we find on average 20 % less associations of GPP extremes with low values of WAI compared to other continents. Instead, cold spells are associated with negative GPP extremes higher-than-average, similarly to Oceania (on average 10 % and 11 % more than random, respectively, Fig. 10, blue bars). Random is here defined as the expected fraction of events attributed to any driver if the variables were unrelated (= 10%). In contrast, in North America more often high

BGD

11, 1869–1907, 2014

## GPP extremes across continents

J. Zscheischler et al.

Title Page

Abstract

Introduction

Conclusions

References

Tables

Figures

◀

▶

◀

▶

Back

Close

Full Screen / Esc

Printer-friendly Version

Interactive Discussion





in 2003 (Ciais et al., 2005) and 2010 (Barriopedro et al., 2011), respectively, and the extreme drought in South Eastern Australia at the beginning of the 21st century, also known as “Big Dry” (Leblanc et al., 2009; Ummenhofer et al., 2009). The good matching between the AVG and well-known events from the literature is encouraging because it demonstrates that averaging different data sets with high uncertainties can result in a reasonably good representation of large-scale extreme events. An example for such an averaging is a recently presented data product of evapotranspiration (ET, Mueller et al., 2013).

### 3.7 Comparison with other data sets

We compare the global patterns of extremes in GPP from the four data sets MTE, MOD17+, LPJmL and OCN with spatiotemporal extremes in other remote sensing products, in particular EVI, FAPAR, and LAI. All these data sets have a three-dimensional (spatiotemporal) structure albeit with different spatial and temporal resolutions, and hence we can apply the extreme event detection method here, as described in Sect. 2.3. Note, however, that units are not transferable into changes in carbon uptake. The patterns for EVI and FAPAR (Fig. 11a and b, respectively) show good agreement with the overall patterns of GPP extreme events (Fig. 5) in Brazil, the Great Plains, Eastern Europe, Tanzania/Kenya, South Africa and South Eastern Australia. The hot spot in the Indus–Ganga Plain (India) is not visible in EVI and FAPAR. LAI shows strongly pronounced extremes in tropical forests (Amazon and Kongo basin, Indonesia, Fig. 11c). LAI values in tropical forests vary over a much wider range compared to other biomes (Liu et al., 2012). This in turn leads to a much larger interannual variability in these areas resulting in larger extremes.

**BGD**

11, 1869–1907, 2014

## GPP extremes across continents

J. Zscheischler et al.

Title Page

Abstract

Introduction

Conclusions

References

Tables

Figures

◀

▶

◀

▶

Back

Close

Full Screen / Esc

Printer-friendly Version

Interactive Discussion



## 4 Conclusions

We present a detailed analysis of spatiotemporal contiguous extremes in different data sets of gross primary productivity (GPP) over the last 30 yr and compare their impacts across continents. We show that the overall impact and spatial extent of extreme events in GPP follow power law distributions and confirm earlier findings that water scarcity has to be regarded as the key driver of negative GPP extremes. However, we identify pronounced regional deviations from this global picture. Depending on the continent, also fires (all continents except North America and Asia), high temperatures (North America), cold spells (Europe and Oceania), and intense precipitation events (South America and Oceania) provoke major decreases in GPP. A comparison of these findings with a literature survey and a validation with remotely sensed data sets including EVI and fAPAR generally supports our identification of the largest GPP extremes, and confirms the reported geographical distributions.

The research on extreme events in both climate variables and vegetation indexes is important to fully understand carbon cycle variability and ultimately carbon cycle–climate feedbacks. While in the past changes in the mean were the primary focus of research, today studies on climate extremes and their impacts on the terrestrial biosphere are mounting. This change in focus might have been driven by the insight that changes in extreme events can alter the functioning of terrestrial ecosystems more strongly than changes in the mean (Jentsch and Beierkuhnlein, 2008). But before accessing *changes* in extremes (including their impacts) we first have to understand how extremes in climate and vegetation are related. In this contribution we corroborate the importance of extreme events for interannual variability of GPP at continental scales. Yet, despite the prominence of water availability as most important driver for extremes in GPP at all continents, the susceptibility to other drivers such as fires and extreme temperatures largely differs across continents. The reason for that might lie in different vulnerabilities of the dominant ecosystems on each continent towards extreme environmental conditions.

BGD

11, 1869–1907, 2014

## GPP extremes across continents

J. Zscheischler et al.

Title Page

Abstract

Introduction

Conclusions

References

Tables

Figures

◀

▶

◀

▶

Back

Close

Full Screen / Esc

Printer-friendly Version

Interactive Discussion



*Acknowledgements.* This study was supported by the projects CARBO-Extreme (grant agreement no. 226701) and GEOCARBON (grant agreement no. 283080) of the European Community's 7th framework program. We thank Sönke Zaehle for providing data from OCN and Martin Jung for providing upscaled fields of GPP (MTE). Natalia Ungelenk helped with the literature review behind Table 1. JZ is part of the International Max Planck Research School for global Biogeochemical Cycles (IMPRS-gBGC).

The service charges for this open access publication have been covered by the Max Planck Society.

## References

- Anderson, L. O., Malhi, Y., Aragão, L. E., Ladle, R., Arai, E., Barbier, N., and Phillips, O.: Remote sensing detection of droughts in Amazonian forest canopies, *New Phytol.*, 187, 733–750, 2010. 1896
- Arnone, J. a., Verburg, P. S. J., Johnson, D. W., Larsen, J. D., Jasoni, R. L., Lucchesi, A. J., Batts, C. M., von Nagy, C., Coulombe, W. G., Schorran, D. E., Buck, P. E., Braswell, B. H., Coleman, J. S., Sherry, R. A., Wallace, L. L., Luo, Y., and Schimel, D. S.: Prolonged suppression of ecosystem carbon dioxide uptake after an anomalously warm year, *Nature*, 455, 383–386, 2008. 1871
- Asner, G. P., Kellner, J. R., Kennedy-Bowdoin, T., Knapp, D. E., Anderson, C., and Martin, R. E.: Forest canopy gap distributions in the southern Peruvian Amazon, *PLoS ONE*, 8, e60875, doi:10.1371/journal.pone.0060875, 2013. 1879
- Baldocchi, D., Falge, E., Gu, L., Olson, R., Hollinger, D., Running, S., Anthoni, P., Bernhofer, C., Davis, K., Evans, R. et al.: FLUXNET: a new tool to study the temporal and spatial variability of ecosystem-scale carbon dioxide, water vapor, and energy flux densities, *B. Am. Meteorol. Soc.*, 82, 2415–2434, 2001. 1873
- Barriopedro, D., Fischer, E. M., Luterbacher, J., Trigo, R. M., and García-Herrera, R.: The hot summer of 2010: redrawing the temperature record map of Europe, *Science*, 332, 220–224, 2011. 1884, 1885, 1896
- Beer, C., Reichstein, M., Tomelleri, E., Ciais, P., Jung, M., Carvalhais, N., Rödenbeck, C., Arain, M. A., Baldocchi, D., Bonan, G. B., Bondeau, A., Cescatti, A., Lasslop, G., Lin-

**BGD**

11, 1869–1907, 2014

## GPP extremes across continents

J. Zscheischler et al.

Title Page

Abstract

Introduction

Conclusions

References

Tables

Figures

◀

▶

◀

▶

Back

Close

Full Screen / Esc

Printer-friendly Version

Interactive Discussion



## GPP extremes across continents

J. Zscheischler et al.

[Title Page](#)[Abstract](#)[Introduction](#)[Conclusions](#)[References](#)[Tables](#)[Figures](#)[◀](#)[▶](#)[◀](#)[▶](#)[Back](#)[Close](#)[Full Screen / Esc](#)[Printer-friendly Version](#)[Interactive Discussion](#)

droth, A., Lomas, M., Luysaert, S., Margolis, H., Oleson, K. W., Roupsard, O., Veenendaal, E., Viovy, N., Williams, C., Woodward, F. I., and Papale, D.: Terrestrial gross carbon dioxide uptake: global distribution and covariation with climate, *Science*, 329, 834–838, 2010. 1874

- 5 Bigler, C., Gavin, D. G., Gunning, C., and Veblen, T. T.: Drought induces lagged tree mortality in a subalpine forest in the Rocky Mountains, *Oikos*, 116, 1983–1994, 2007. 1871
- Bollobas, B. and Riordan, O.: *Percolation*, Cambridge University Press, Cambridge, 2006. 1880
- Bondeau, A., Smith, P. C., Zaehle, S., Schaphoff, S., Lucht, W., Cramer, W., Gerten, D., Lotze-Campen, H., Müller, C., Reichstein, M., and Smith, B.: Modelling the role of agriculture for the 20th century global terrestrial carbon balance, *Glob. Change Biol.*, 13, 679–706, 2007. 1874
- 10 Bréda, N., Huc, R., Granier, A., and Dreyer, E.: Temperate forest trees and stands under severe drought: a review of ecophysiological responses, adaptation processes and long-term consequences, *Ann. For. Sci.*, 63, 625–644, 2006. 1871
- 15 Ciais, P., Reichstein, M., Viovy, N., Granier, A., Ogée, J., Allard, V., Aubinet, M., Buchmann, N., Bernhofer, C., Carrara, A., Chevallier, F., De Noblet, N., Friend, A. D., Friedlingstein, P., Grünwald, T., Heinesch, B., Keronen, P., Knohl, A., Krinner, G., Loustau, D., Manca, G., Matteucci, G., Miglietta, F., Ourcival, J. M., Papale, D., Pilegaard, K., Rambal, S., Seufert, G., Soussana, J. F., Sanz, M. J., Schulze, E. D., Vesala, T., and Valentini, R.: Europe-wide reduction in primary productivity caused by the heat and drought in 2003, *Nature*, 437, 529–533, 2005. 1871, 1885, 1896
- 20 Clauset, A., Shalizi, C. R., and Newman, M. E. J.: Power-law distributions in empirical data, *SIAM Rev.*, 51, 661–703, 2009. 1877
- Coles, S.: *An Introduction to Statistical Modeling of Extreme Values*, Springer, London, 2001. 1872
- 25 Coumou, D. and Rahmstorf, S.: A decade of weather extremes, *Nat. Clim. Change*, 2, 491–496, 2012. 1884, 1896
- Dee, D., Uppala, S., Simmons, A., Berrisford, P., Poli, P., Kobayashi, S., Andrae, U., Balmaseda, M., Balsamo, G., Bauer, P., Bechtold, P., Beljaars, A. C. M., van de Berg, L., Bidlot, J., Bormann, N., Delsol, C., Dragani, R., Fuentes, M., Geer, A. J., Haimberger, L., Healy, S. B., Hersbach, H., Hólm, E. V., Isaksen, L., Kållberg, P., Köhler, M., Matricardi, M., McNally, A. P., Monge-Sanz, B. M., Morcrette, J.-J., Park, B.-K., Peubey, C., de Rosnay, P., Tavolato, C.,
- 30

## GPP extremes across continents

J. Zscheischler et al.

Title Page

Abstract

Introduction

Conclusions

References

Tables

Figures

◀

▶

◀

▶

Back

Close

Full Screen / Esc

Printer-friendly Version

Interactive Discussion



Thépaut, J.-N., and Vitart, F.: The ERA-Interim reanalysis: configuration and performance of the data assimilation system, *Q. J. Roy. Meteor. Soc.*, 137, 553–597, 2011. 1874, 1875

Dong, X., Xi, B., Kennedy, A., Feng, Z., Entin, J. K., Houser, P. R., Schiffer, R. A., L'Ecuyer, T., Olson, W. S., Hsu, K.-L., Liu, W. T., Lin, B., Deng, Y., and Jiang, T.: Investigation of the 2006 drought and 2007 flood extremes at the Southern Great Plains through an integrative analysis of observations, *J. Geophys. Res.-Atmos.*, 116, D03204, doi:10.1029/2010JD014776, 2011. 1896

Farquhar, G., Caemmerer, S., and Berry, J.: A biochemical model of photosynthetic CO<sub>2</sub> assimilation in leaves of C3 species, *Planta*, 149, 78–90, 1980. 1874

Field, R. D., van der Werf, G. R., and Shen, S. S. P.: Human amplification of drought-induced biomass burning in Indonesia since 1960, *Nat. Geosci.*, 2, 185–188, 2009. 1871

Fisher, J. I., Hurtt, G. C., Thomas, R. Q., and Chambers, J. Q.: Clustered disturbances lead to bias in large-scale estimates based on forest sample plots, *Ecol. Lett.*, 11, 554–563, doi:10.1111/j.1461-0248.2008.01169.x, 2008. 1879

Friend, A. D. and Kiang, N. Y.: Land surface model development for the GISS GCM: effects of improved canopy physiology on simulated climate, *J. Climate*, 18, 2883–2902, 2005. 1874

Galvin, K. A., Boone, R. B., Smith, N. M., and Lynn, S. J.: Impacts of climate variability on East African pastoralists: linking social science and remote sensing, *Clim. Res.*, 19, 161–172, 2001. 1896

Gerten, D., Schaphoff, S., Haberlandt, U., Lucht, W., and Sitch, S.: Terrestrial vegetation and water balance – hydrological evaluation of a dynamic global vegetation model, *J. Hydrol.*, 286, 249–270, 2004. 1874

Ghil, M., Yiou, P., Hallegatte, S., Malamud, B. D., Naveau, P., Soloviev, A., Friederichs, P., Keilis-Borok, V., Kondrashov, D., Kossobokov, V., Mestre, O., Nicolis, C., Rust, H. W., Shebalin, P., Vac, M., Witt, A., and Zaliapin, I.: Extreme events: dynamics, statistics and prediction, *Non-linear Proc. Geoph.*, 18, 295–350, 2011. 1872

Giglio, L., Randerson, J. T., van der Werf, G. R., Kasibhatla, P. S., Collatz, G. J., Morton, D. C., and DeFries, R. S.: Assessing variability and long-term trends in burned area by merging multiple satellite fire products, *Biogeosciences*, 7, 1171–1186, doi:10.5194/bg-7-1171-2010, 2010. 1875

Gloor, M., Phillips, O. L., Lloyd, J. J., Lewis, S. L., Malhi, Y., Baker, T. R., López-Gonzalez, G., Peacock, J., Almeida, S., de Oliveira, A. C. A., Alvarez, E., Amaral, I., Arroyo, L., Aymard, G., Banki, O., Blanc, L., Bonal, D., Brando, P., Chao, K.-J., Chave, J., Dávila, N., Erwin, T.,

## GPP extremes across continents

J. Zscheischler et al.

Title Page

Abstract

Introduction

Conclusions

References

Tables

Figures

◀

▶

◀

▶

Back

Close

Full Screen / Esc

Printer-friendly Version

Interactive Discussion



Silva, J., Di Fiore, A., Feldpausch, T. R., Freitas, A., Herrera, R., Higuchi, N., Honorio, E., Jiménez, E., Killeen, T., Laurance, W., Mendoza, C., Monteagudo, A., Andrade, A., Neill, D., Nepstad, D., Vargas, P. N. N., Peñuela, M. C., Cruz, A. P. N., Prieto, A., Pitman, N., Quezada, C., Salomão, R., Silveira, M., Schwarz, M., Stropp, J., Ramírez, F., Ramírez, H., Rudas, A., ter Steege, H., Silva, N., Torres, A., Terborgh, J., Vásquez, R., and van der Heijden, G.: Does the disturbance hypothesis explain the biomass increase in basin-wide Amazon forest plot data?, *Glob. Change Biol.*, 15, 2418–2430, 2009. 1879

Gumbel, E.: *Statistics of Extremes*, Dover Publications, Dover, 2004. 1872

Haxeltine, A. and Prentice, I.: A general model for the light-use efficiency of primary production, *Funct. Ecol.*, 10, 551–561, 1996. 1874

Huete, A., Didan, K., Miura, T., Rodriguez, E., Gao, X., and Ferreira, L.: Overview of the radiometric and biophysical performance of the MODIS vegetation indices, *Remote Sens. Environ.*, 83, 195–213, 2002. 1875

IPCC: *Managing the Risks of Extreme Events and Disasters to Advance Climate Change Adaptation*, A Special Report of Working Groups I and II of the Intergovernmental Panel on Climate Change, edited by: Field, C. B., Barros, V., Stocker, T. F., Qin, D., Dokken, D. J., Ebi, K. L., Mastrandrea, M. D., Mach, K. J., Plattner, G.-K., Allen, S. K., Tignor, M., and Midgley, P. M., Cambridge University Press, Cambridge, UK, and New York, NY, USA, 2012. 1872, 1875

Irland, L. C.: Ice storms and forest impacts, *Sci. Total Environ.*, 262, 231–242, 2000. 1871

Jentsch, A. and Beierkuhnlein, C.: Research frontiers in climate change: effects of extreme meteorological events on ecosystems, *C. R. Geosci.*, 340, 621–628, 2008. 1886

Jung, M., Reichstein, M., Margolis, H., Cescatti, A., Richardson, A., Arain, M., Arneeth, A., Bernhofer, C., Bonal, D., Chen, J., Gianelle, D., Gobron, N., Kiely, G., Kutsch, W., Lasslop, G., E., L. B., Lindroth, A., Merbold, L., Montagnani, L., Moors, E. J., Papale, D., Sottocornola, M., Vaccari, F., and Williams, C.: Global patterns of land-atmosphere fluxes of carbon dioxide, latent heat, and sensible heat derived from eddy covariance, satellite, and meteorological observations, *J. Geophys. Res.*, 116, G00J07, doi:10.1029/2010JG001566, 2011. 1873, 1874, 1875, 1881

Keenan, T., Baker, I., Barr, A., Ciais, P., Davis, K., Dietze, M., Dragoni, D., Gough, C. M., Grant, R., Hollinger, D., Hufkens, K., Poulter, B., McCaughey, H., Raczka, B., Ryu, Y., Schaefer, K., Tian, H., Verbeeck, H., Zhao, M., and Richardson, A. D.: Terrestrial biosphere model performance for inter-annual variability of land-atmosphere CO<sub>2</sub> exchange, *Glob. Change Biol.*, 18, 1971–1987, 2012. 1881

## GPP extremes across continents

J. Zscheischler et al.

Title Page

Abstract

Introduction

Conclusions

References

Tables

Figures

◀

▶

◀

▶

Back

Close

Full Screen / Esc

Printer-friendly Version

Interactive Discussion



- Kéfi, S., Rietkerk, M., Alados, C. L., Pueyo, Y., Papanastasis, V. P., ElAich, A., and De Ruiter, P. C.: Spatial vegetation patterns and imminent desertification in Mediterranean arid ecosystems, *Nature*, 449, 213–217, 2007. 1879
- Kellner, J. R. and Asner, G. P.: Convergent structural responses of tropical forests to diverse disturbance regimes, *Ecol. Lett.*, 12, 887–97, 2009. 1879
- 5 Krinner, G., Viovy, N., de Noblet-Ducoudré, N., Ogée, J., Polcher, J., Friedlingstein, P., Ciais, P., Sitch, S., and Prentice, I. C.: A dynamic global vegetation model for studies of the coupled atmosphere-biosphere system, *Global Biogeochem. Cy.*, 19, GB1015, doi:10.1029/2003GB002199, 2005. 1874
- 10 Kurz, W. A., Dymond, C. C., Stinson, G., Rampley, G. J., Neilson, E. T., Carroll, A. L., Ebata, T., and Safranyik, L.: Mountain pine beetle and forest carbon feedback to climate change, *Nature*, 452, 987–990, 2008. 1871
- Leblanc, M. J., Tregoning, P., Ramillien, G., Tweed, S. O., and Fakes, A.: Basin-scale, integrated observations of the early 21st century multiyear drought in southeast Australia, *Water Resour. Res.*, 45, W04408, doi:10.1029/2008WR007333, 2009. 1885, 1896
- 15 Leonard, M., Westra, S., Phatak, A., Lambert, M., van den Hurk, B., McInnes, K., Risbey, J., Schuster, S., Jakob, D., and Stafford-Smith, M.: A compound event framework for understanding extreme impacts, *Wiley Interdisciplinary Reviews: Climate Change*, 2013. 1872, 1884
- Lewis, S. L., Brando, P. M., Phillips, O. L., van der Heijden, G. M. F., and Nepstad, D.: The 2010 Amazon drought, *Science*, 331, p. 554, 2011. 1884, 1896
- 20 Liu, Y., Liu, R., and Chen, J. M.: Retrospective retrieval of long-term consistent global leaf area index (1981–2011) from combined AVHRR and MODIS data, *J. Geophys. Res.-Biogeo.*, 117, G04003, doi:10.1029/2012JG002084, 2012. 1875, 1885
- Lloyd-Hughes, B.: A spatio-temporal structure-based approach to drought characterisation, *Int. J. Climatol.*, 32, 406–418, 2012. 1873, 1876
- 25 Marquet, P. A., Navarrete, S. A., and Castilla, J. C.: Scaling population density to body size in rocky intertidal communities, *Science*, 250, 1125–1127, 1990. 1879
- Minetti, J. L., Vargas, W. M., Poblete, A., Acuña, L., and Casagrande, G.: Non-linear trends and low frequency oscillations in annual precipitation over Argentina and Chile, 1931–1999, *Atmósfera*, 16, 119–135, 2009. 1896
- 30 Morse, D., Lawton, J., Dodson, M., and Williamson, M.: Fractal dimension of vegetation and the distribution of arthropod body lengths, *Nature*, 314, 731–733, 1985. 1879

## GPP extremes across continents

J. Zscheischler et al.

Title Page

Abstract

Introduction

Conclusions

References

Tables

Figures

◀

▶

◀

▶

Back

Close

Full Screen / Esc

Printer-friendly Version

Interactive Discussion



- Mueller, B., Hirschi, M., Jimenez, C., Ciais, P., Dirmeyer, P. A., Dolman, A. J., Fisher, J. B., Jung, M., Ludwig, F., Maignan, F., Miralles, D. G., McCabe, M. F., Reichstein, M., Sheffield, J., Wang, K., Wood, E. F., Zhang, Y., and Seneviratne, S. I.: Benchmark products for land evapotranspiration: LandFlux-EVAL multi-data set synthesis, *Hydrol. Earth Syst. Sci.*, 17, 3707–3720, doi:10.5194/hess-17-3707-2013, 2013. 1885
- 5 Myneni, R. B., Los, S. O., and Tucker, C. J.: Satellite-based identification of linked vegetation index and sea surface temperature Anomaly areas from 1982–1990 for Africa, Australia and South America, *Geophys. Res. Lett.*, 23, 729–732, 1996. 1896
- Namias, J.: Spring and summer 1988 drought over the contiguous United States – causes and prediction, *J. Climate*, 4, 54–65, 1991. 1896
- 10 Negrón-Juárez, R. and Chambers, J.: Widespread Amazon forest tree mortality from a single cross-basin squall line event, *Geophys. Res.*, 37, 1–5, 2010. 1871
- Newman, M. E. J.: Power laws, Pareto distributions and Zipf’s law, *Contemp. Phys.*, 46, 323–351, 2005. 1880
- 15 Page, S. E., Siegert, F., Rieley, J. O., Boehm, H.-D. V., Jayak, A., and Limink, S.: The amount of carbon released from peat and forest fires in Indonesia during 1997, *Nature*, 420, 61–65, 2002. 1871
- Pascual, M. and Guichard, F.: Criticality and disturbance in spatial ecological systems, *Trends Ecol. Evol.*, 20, 88–95, 2005. 1880
- 20 Phillips, O., Aragão, L., Lewis, S., and Fisher, J.: Drought sensitivity of the Amazon rainforest, *Science*, 323, 1344–1347, 2009. 1871
- Piao, S., Sitch, S., Ciais, P., Friedlingstein, P., Peylin, P., Wang, X., Ahlström, A., Anav, A., Canadell, J. G., Cong, N., Huntingford, C., Jung, M., Levis, S., Levy, P. E., Li, J., Lin, X., Lomas, M. R., Lu, M., Luo, Y., Ma, Y., Myneni, R. B., Poulter, B., Sun, Z., Wang, T., Viovy, N., Zaehle, S., and Zeng, N.: Evaluation of terrestrial carbon cycle models for their response to climate variability and to CO<sub>2</sub> trends, *Glob. Change Biol.*, 19, 2117–2132, 2013. 1881
- 25 Prentice, C. I., Sykes, M. T., and Cramer, W.: A simulation model for the transient effects of climate change on forest landscapes, *Ecol. Model.*, 65, 51–70, 1993. 1875
- Pueyo, S., de Alencastro Graça, P. M. L., Barbosa, R. I., Cots, R., Cardona, E., and Fearnside, P. M.: Testing for criticality in ecosystem dynamics: the case of Amazonian rainforest and savanna fire, *Ecol. Lett.*, 13, 793–802, 2010. 1880
- 30 Rao, V. B., Hada, K., and Herdies, D. L.: On the severe drought of 1993 in north-east Brazil, *Int. J. Climatol.*, 15, 697–704, 1995. 1896

## GPP extremes across continents

J. Zscheischler et al.

Title Page

Abstract

Introduction

Conclusions

References

Tables

Figures

◀

▶

◀

▶

Back

Close

Full Screen / Esc

Printer-friendly Version

Interactive Discussion



- Reichstein, M., Ciais, P., Papale, D., Valentini, R., Running, S., Viovy, N., Cramer, W., Granier, A., Ogee, J., Allard, V., Aubinet, M., Bernhofer, C., Buchmann, N., Carrara, A., Grünwald, T., Heimann, M., Heinesch, B., Knohl, A., Kutsch, W., Loustau, D., Manca, G., Matteucci, G., Miglietta, F., Ourcival, J., Pilegaard, K., Pumpanen, J., Rambal, S., Schaphoff, S., Seufert, G., Soussana, J.-F., Sanz, M.-J., Vesala, T., and Zhao, M.: Reduction of ecosystem productivity and respiration during the European summer 2003 climate anomaly: a joint flux tower, remote sensing and modelling analysis, *Glob. Change Biol.*, 13, 634–651, 2007. 1871
- Reichstein, M., Bahn, M., Ciais, P., Mahecha, M. D., Seneviratne, S. I., Zscheischler, J., Beer, C., Buchmann, N., Frank, D., Papale, D., Rammig, A., Smith, P., Thonicke, K., van der Velde, M., Vicca, S., Walz, A., and Wattenbach, M.: Climate extremes and the carbon cycle, *Nature*, 500, 287–295, 2013. 1870, 1872, 1873, 1880, 1883, 1884
- Rojas, O., Vrieling, A., and Rembold, F.: Assessing drought probability for agricultural areas in Africa with coarse resolution remote sensing imagery, *Remote Sens. Environ.*, 115, 343–352, 2011. 1896
- Rouault, M. and Richard, Y.: Intensity and spatial extension of drought in South Africa at different time scales, *Water SA*, 29, 489–500, 2003. 1896
- Running, S. W., Thornton, P. E., Nemani, R., and Glassy, J. M.: Global terrestrial gross and net primary productivity from the Earth Observing System, in: *Methods in Ecosystem Science*, 44–57, 2000. 1874
- Running, S. W., Nemani, R. R., Heinsch, F. A., Zhao, M., Reeves, M., and Hashimoto, H.: A continuous satellite-derived measure of global terrestrial primary production, *Bioscience*, 54, 547–560, 2004. 1873, 1875
- Seneviratne, S. I., Nicholls, N., Easterling, D., Goodess, C., Kanae, S., Kossin, J., Luo, Y., Marengo, J., McInnes, K., Rahimi, M., Reichstein, M., Sorteberg, A., Vera, C., and Zhang, X.: Changes in climate extremes and their impacts on the natural physical environment, in: *Managing the Risks of Extreme Events and Disasters to Advance Climate Change Adaptation (IPCC SREX Report)*, edited by: Field, C. B. et al., 109–230, 2012. 1876, 1884
- Sitch, S., Smith, B., Prentice, I. C., Arneeth, A., Bondeau, A., Cramer, W., Kaplan, J. O., Levis, S., Lucht, W., Sykes, M. T., Thonicke, K., and Venevsky, S.: Evaluation of ecosystem dynamics, plant geography and terrestrial carbon cycling in the LPJ dynamic global vegetation model, *Glob. Change Biol.*, 9, 161–185, 2003. 1873, 1874
- Siwkcki, R. and Ufnalski, K.: Review of oak stand decline with special reference to the role of drought in Poland, *Eur. J. Forest Pathol.*, 28, 99–112, 1998. 1896

- Smith, M. D.: An ecological perspective on extreme climatic events: a synthetic definition and framework to guide future research, *J. Ecol.*, 99, 656–663, 2011. 1872
- Sornette, D.: *Critical Phenomena in Natural Sciences: Chaos, Fractals, Selforganization and Disorder*, Springer, 2006. 1880
- 5 Sun, Y., Gu, L., Dickinson, R. E., and Zhou, B.: Forest greenness after the massive 2008 Chinese ice storm: integrated effects of natural processes and human intervention, *Environ. Res. Lett.*, 7, 035702, doi:10.1088/1748-9326/7/3/035702, 2012. 1871
- Thonicke, K., Spessa, A., Prentice, I. C., Harrison, S. P., Dong, L., and Carmona-Moreno, C.: The influence of vegetation, fire spread and fire behaviour on biomass burning and trace gas emissions: results from a process-based model, *Biogeosciences*, 7, 1991–2011, doi:10.5194/bg-7-1991-2010, 2010. 1874
- 10 Touboul, J. and Destexhe, A.: Can power-law scaling and neuronal avalanches arise from stochastic dynamics?, *PLoS One*, 5, e8982, doi:10.1371/journal.pone.0008982, 2010. 1880
- 15 Turcotte, D. L., Malamud, B. D., Guzzetti, F., and Reichenbach, P.: Self-organization, the cascade model, and natural hazards, *P. Natl. Acad. Sci. USA*, 99, 2530–2537, 2002. 1879
- Ummenhofer, C. C., England, M. H., McIntosh, P. C., Meyers, G. A., Pook, M. J., Risbey, J. S., Gupta, A. S., and Taschetto, A. S.: What causes southeast Australia's worst droughts?, *Geophys. Res. Lett.*, 36, L04706, doi:10.1029/2008GL036801, 2009. 1885
- 20 Varadhan, S. R. S.: Asymptotic probabilities and differential equations, *Commun. Pur. Appl. Math.*, 19, 261–286, 1966. 1880
- Waple, A. and Lawrimore, J.: State of the climate in 2002, *B. Am. Meteorol. Soc.*, 84, 800–800, 2003. 1896
- Westerling, A. L., Hidalgo, H. G., Cayan, D. R., and Swetnam, T. W.: Warming and earlier spring increase western US forest wildfire activity, *Science*, 313, 940–943, 2006. 1871
- 25 Zaehle, S. and Friend, A. D.: Carbon and nitrogen cycle dynamics in the O-CN land surface model: 1. Model description, site-scale evaluation, and sensitivity to parameter estimates, *Global Biogeochem. Cy.*, 24, GB1005, doi:10.1029/2009GB003521, 2010. 1873
- Zeng, H., Chambers, J. Q., Negrón-Juárez, R. I., Hurtt, G. C., Baker, D. B., and Powell, M. D.: Impacts of tropical cyclones on US forest tree mortality and carbon flux from 1851 to 2000, *P. Natl. Acad. Sci. USA*, 106, 7888–7892, 2009. 1871
- 30 Zhao, M. and Running, S. W.: Drought-induced reduction in global terrestrial net primary production from 2000 through 2009, *Science*, 329, 940–943, 2010. 1871

---

**GPP extremes across continents**J. Zscheischler et al.

---

[Title Page](#)[Abstract](#)[Introduction](#)[Conclusions](#)[References](#)[Tables](#)[Figures](#)[◀](#)[▶](#)[◀](#)[▶](#)[Back](#)[Close](#)[Full Screen / Esc](#)[Printer-friendly Version](#)[Interactive Discussion](#)

Zscheischler, J., Mahecha, M. D., Harmeling, S., and Reichstein, M.: Detection and attribution of large spatiotemporal extreme events in Earth observation data, *Ecol. Inform.*, 15, 66–73, 2013. 1873, 1875, 1878, 1879

Zscheischler, J., Mahecha, M. D., von Buttlar, J., Harmeling, S., Jung, M., Rammig, A., Rander-son, J., Schölkopf, B., Seneviratne, S. I., Tomelleri, E., Zaehle, S., and Reichstein, M.: Few extremes dominate interannual variability in gross primary production, *Environ. Res. Lett.*, 9, in press, 2014. 1872, 1873, 1879, 1880, 1881, 1882, 1883, 1897, 1901

720

## BGD

11, 1869–1907, 2014

### GPP extremes across continents

J. Zscheischler et al.

[Title Page](#)

[Abstract](#)

[Introduction](#)

[Conclusions](#)

[References](#)

[Tables](#)

[Figures](#)

[I ◀](#)

[▶ I](#)

[◀](#)

[▶](#)

[Back](#)

[Close](#)

[Full Screen / Esc](#)

[Printer-friendly Version](#)

[Interactive Discussion](#)



## GPP extremes across continents

J. Zscheischler et al.

**Table 1.** Approximate location, timing and literature for the largest negative 1st-percentile GPP extreme event at each of the five data sets MTE, MOD17+, LPJmL, OCN and AVG on each continent.

	MTE	MOD17+	LPJmL	OCN	AVG
NA where what ref	2011 Texas, South West US drought (Coumou and Rahmstorf, 2012)	1988 Midwestern US drought (Namias, 1991)	2006 Great Plains drought (Dong et al., 2011)	2006 Great Plains drought (Dong et al., 2011)	2011 Texas, South West US drought (Coumou and Rahmstorf, 2012)
SA where what ref	1992–1993 NE Brazil drought (Rao et al., 1995)	2010 Amazon drought (Lewis et al., 2011)	1995–1996 Northern Argentina drought (Minetti et al., 2009)	2004–2006 Eastern Amazon drought (Anderson et al., 2010)	2010 SE Amazon drought (Lewis et al., 2011)
EU where what ref	1987 Eastern Europe	2003 Central Europe drought, heat wave (Ciais et al., 2005)	1992 Central Eastern Europe drought (Siwkcki and Ufnalski, 1998)	2002 South Western Russia cold spell, flooding (Waple and Lawrimore, 2003)	2003 Central Europe drought, heat wave (Ciais et al., 2005)
AF where what ref	1984–1985 Sahel drought, famine (Rojas et al., 2011)	1996–1997 East Africa drought (Galvin et al., 2001)	1992 South Africa drought (Rouault and Richard, 2003)	1991–1994 East Africa drought (Galvin et al., 2001)	1996–1997 East Africa drought (Galvin et al., 2001)
AS where what ref	2010 Russia heat wave (Barriopedro et al., 2011)	2010 Russia heat wave (Barriopedro et al., 2011)	2010 Russia heat wave (Barriopedro et al., 2011)	2010 Russia heat wave (Barriopedro et al., 2011)	2010 Russia heat wave (Barriopedro et al., 2011)
OC where what ref	2002–2003 SE Australia Millennium drought (Leblanc et al., 2009)	2002–2004 Eastern Malaysia	1982–1983 SE Australia drought (Myneni et al., 1996)	1982–1983 SE Australia drought (Myneni et al., 1996)	2002–2003 SE Australia Millennium drought (Leblanc et al., 2009)

Title Page

Abstract

Introduction

Conclusions

References

Tables

Figures

◀

▶

◀

▶

Back

Close

Full Screen / Esc

Printer-friendly Version

Interactive Discussion



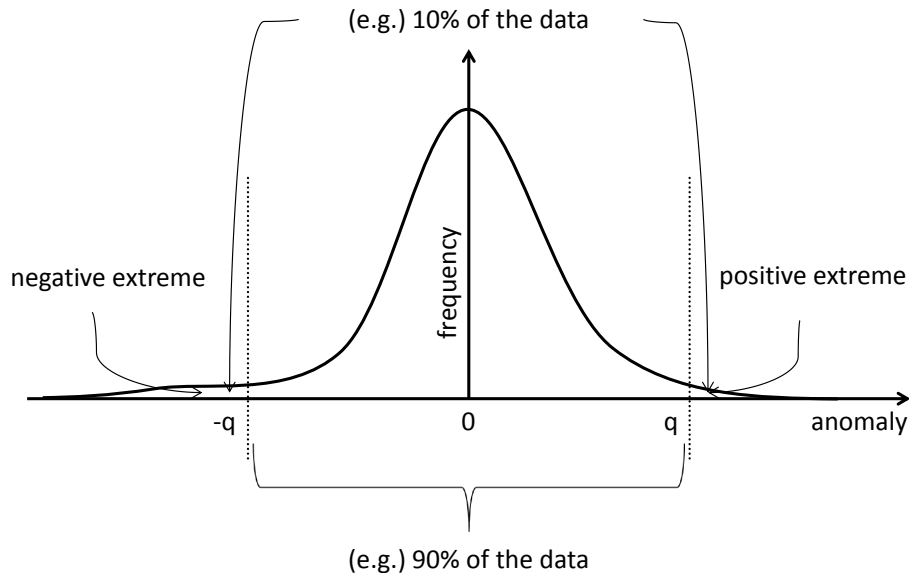


**Fig. 1.** Sketch of how extremes are defined on GPP anomalies. A symmetric threshold  $q$  is set such that (e.g.) 90% of the data anomalies fall in between  $-q$  and  $q$ . Those values which exceed the threshold are defined to be extreme. In this example the extremes are defined using the 10th-percentile definition (not to scale). Reprint of Fig. A2 in Zscheischler et al. (2014).

**GPP extremes across continents**

J. Zscheischler et al.

<a href="#">Title Page</a>	
<a href="#">Abstract</a>	<a href="#">Introduction</a>
<a href="#">Conclusions</a>	<a href="#">References</a>
<a href="#">Tables</a>	<a href="#">Figures</a>
<a href="#">◀</a>	<a href="#">▶</a>
<a href="#">◀</a>	<a href="#">▶</a>
<a href="#">Back</a>	<a href="#">Close</a>
<a href="#">Full Screen / Esc</a>	
<a href="#">Printer-friendly Version</a>	
<a href="#">Interactive Discussion</a>	



## GPP extremes across continents

J. Zscheischler et al.

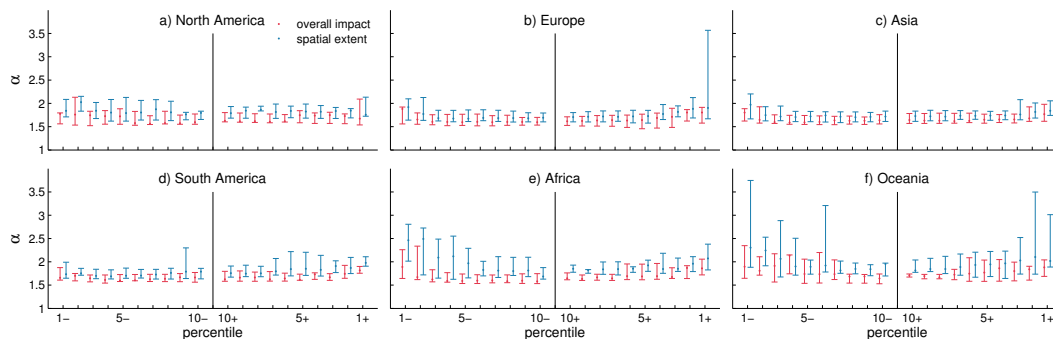


**Fig. 2.** Values of the power law exponent  $\alpha$  for the overall impact (blue) and spatial extent (red) of extremes in GPP. Shown are the median (dot) and the range of the data sets MTE, MOD17+, LPJmL, OCN and AVG for the positive (+) and negative(–) extremes for the percentiles 1 to 10.

Title Page

Abstract

Introduction

Conclusions

References

Tables

Figures

◀

▶

◀

▶

Back

Close

Full Screen / Esc

Printer-friendly Version

Interactive Discussion



## GPP extremes across continents

J. Zscheischler et al.

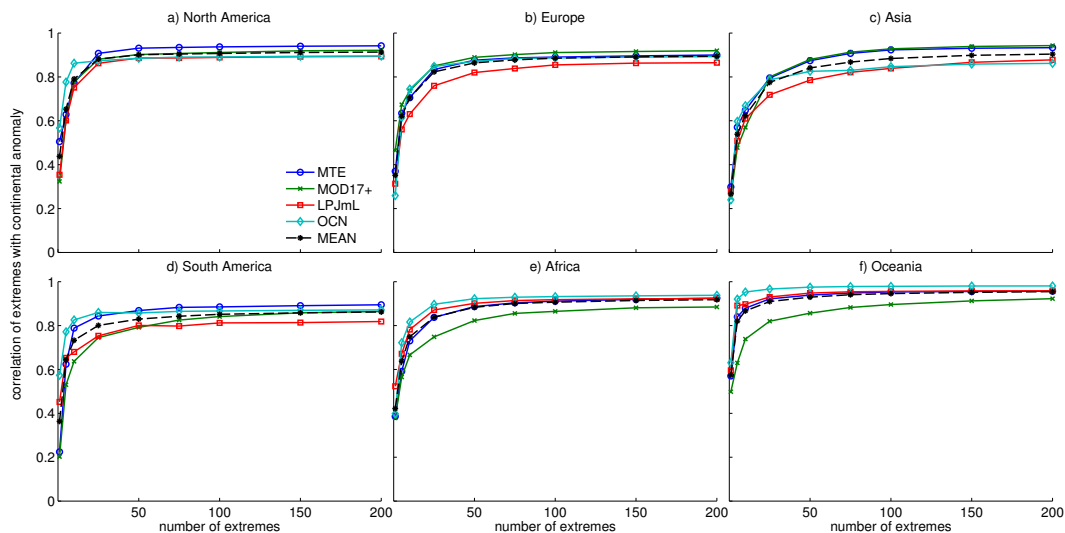


**Fig. 3.** Correlations of 10th-percentile extremes (positive and negative) with aggregated anomalies on each continent. Depicted are the correlation coefficients for the data sets MTE (blue circles), MOD17+ (green cross), LPLPJM (red square), OCN (cyan diamond). The dashed black line shows the mean of the correlation coefficients of the four data sets.

Title Page

Abstract

Introduction

Conclusions

References

Tables

Figures

◀

▶

◀

▶

Back

Close

Full Screen / Esc

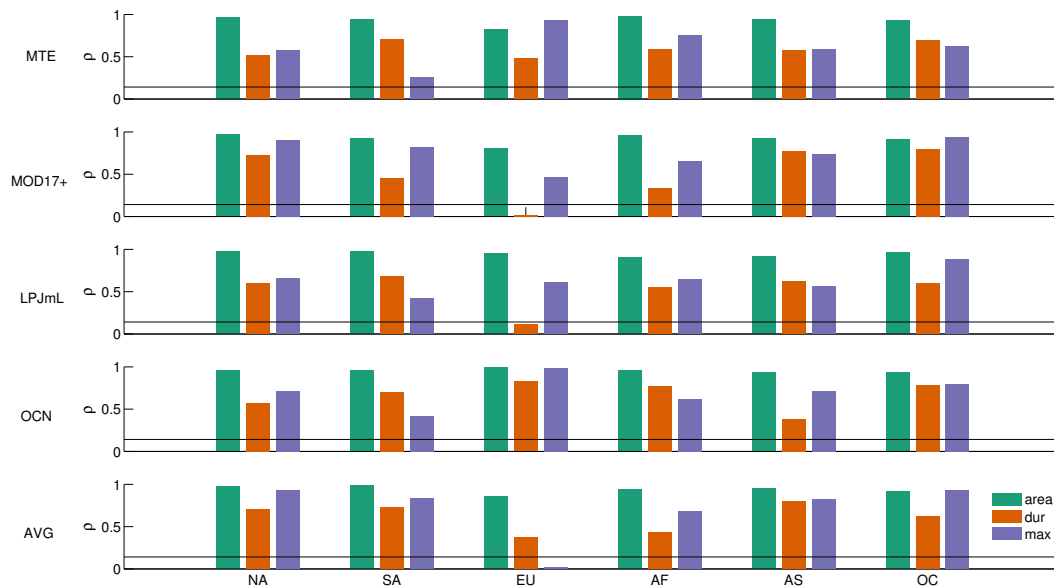
Printer-friendly Version

Interactive Discussion



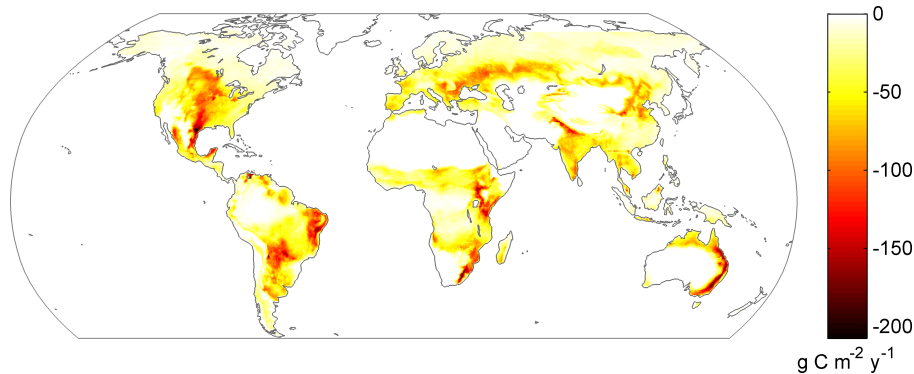
## GPP extremes across continents

J. Zscheischler et al.



**Fig. 4.** Correlations of spatial extent (green), duration (orange) and maximal anomaly (purple) of GPP extreme events with their overall impacts. Depicted are the correlations of extremes on all continents and the data sets MTE, MOD17+, LPJmL, OCN and AVG.

[Title Page](#)
[Abstract](#)
[Introduction](#)
[Conclusions](#)
[References](#)
[Tables](#)
[Figures](#)
[◀](#)
[▶](#)
[◀](#)
[▶](#)
[Back](#)
[Close](#)
[Full Screen / Esc](#)
[Printer-friendly Version](#)
[Interactive Discussion](#)

**Fig. 5.** Global averaged map of negative 10th-percentile extreme events in GPP. The largest 200 10th-percentile extremes in GPP for each continent and the four data sets MTE, MOD17+, LPJmL and OCN were computed and then averaged to obtain the typical impact of GPP extreme events per year. Compare with Fig. 3a in Zscheischler et al. (2014) for an analysis at the global scale.

**GPP extremes across continents**

J. Zscheischler et al.

[Title Page](#)

[Abstract](#)   [Introduction](#)

[Conclusions](#)   [References](#)

[Tables](#)   [Figures](#)

[◀](#)   [▶](#)

[◀](#)   [▶](#)

[Back](#)   [Close](#)

[Full Screen / Esc](#)

[Printer-friendly Version](#)

[Interactive Discussion](#)



## GPP extremes across continents

J. Zscheischler et al.

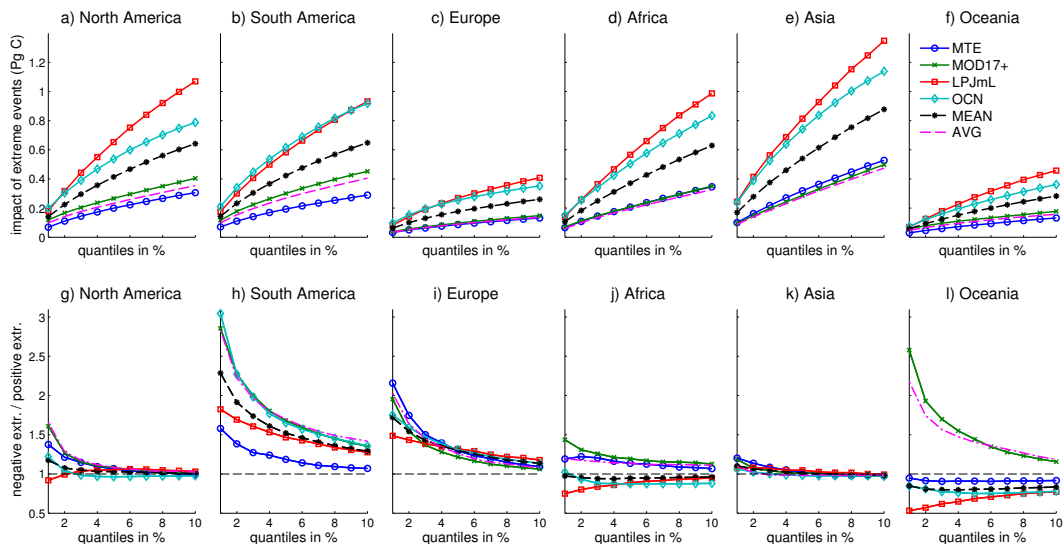


**Fig. 6.** Overall impact and asymmetry of GPP extreme events. Depicted are the 4 different GPP data sets (MTE, MOD17+, LPJmL, OCN), the average of the results of the four (MEAN), and the results for the averaged data set (AVG). **(a–f)** Sum of the overall impact of the largest 200 extreme events in GPP for each continent using the percentiles 1 to 10. **(g–l)** Quotient between 200 largest negative and 200 largest positive extreme events in GPP for each continent using different the percentiles 1 to 10.

Title Page

Abstract

Introduction

Conclusions

References

Tables

Figures

◀

▶

◀

▶

Back

Close

Full Screen / Esc

Printer-friendly Version

Interactive Discussion



## GPP extremes across continents

J. Zscheischler et al.

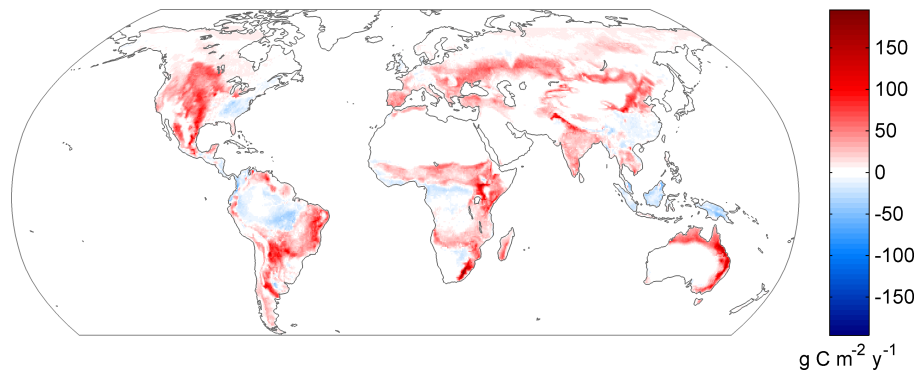


**Fig. 7.** Difference between negative GPP extreme events of the averaged data set AVG and averaged negative GPP extreme events of the four data sets MTE, MOD17+, LPJmL, and OCN. Depicted is the difference in impact per year. For each continent and each data set the 200 largest negative 10th-percentile GPP extreme events were computed and then integrated over time. Red areas imply smaller extreme events in AVG (less negative impact).

Title Page

Abstract

Introduction

Conclusions

References

Tables

Figures

◀

▶

◀

▶

Back

Close

Full Screen / Esc

Printer-friendly Version

Interactive Discussion



**GPP extremes across continents**

J. Zscheischler et al.

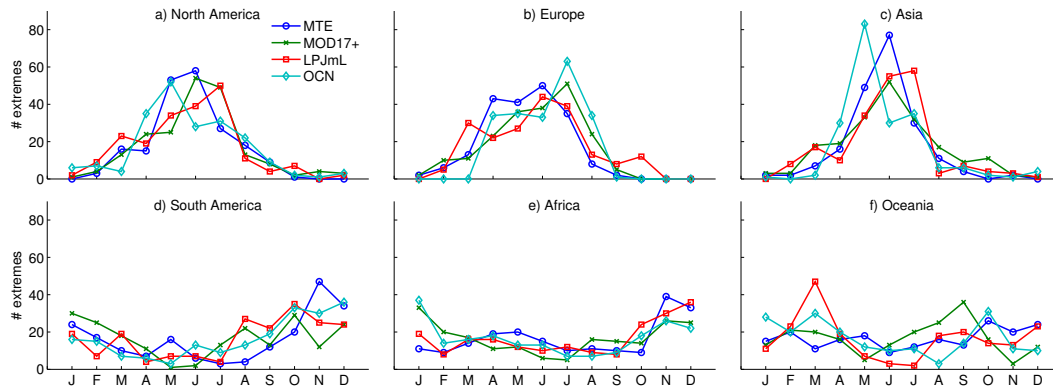


**Fig. 8.** Number of GPP extreme events starting per month for the largest 200 1st-percentile extremes in GPP for each continent and the data sets MTE, MOD17+, LPJmL, OCN.

[Title Page](#)

[Abstract](#)   [Introduction](#)

[Conclusions](#)   [References](#)

[Tables](#)   [Figures](#)

[◀](#)   [▶](#)

[◀](#)   [▶](#)

[Back](#)   [Close](#)

[Full Screen / Esc](#)

[Printer-friendly Version](#)

[Interactive Discussion](#)



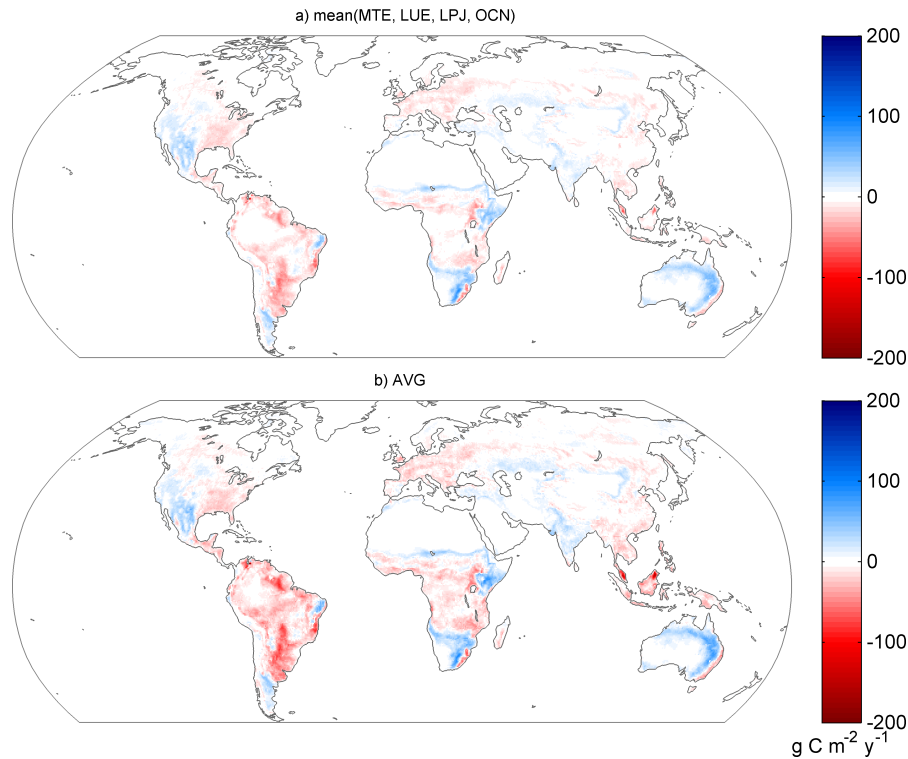


**Fig. 9.** Pixelwise difference between the 200 largest positive and the 200 largest negative extreme events. In the red areas negative extremes dominate. **(a)** Averaged difference between GPP extreme events in the four data sets MTE, MOD17+, LPJmL and OCN. **(b)** Difference between GPP extreme events in the averaged data set AVG.

## GPP extremes across continents

J. Zscheischler et al.

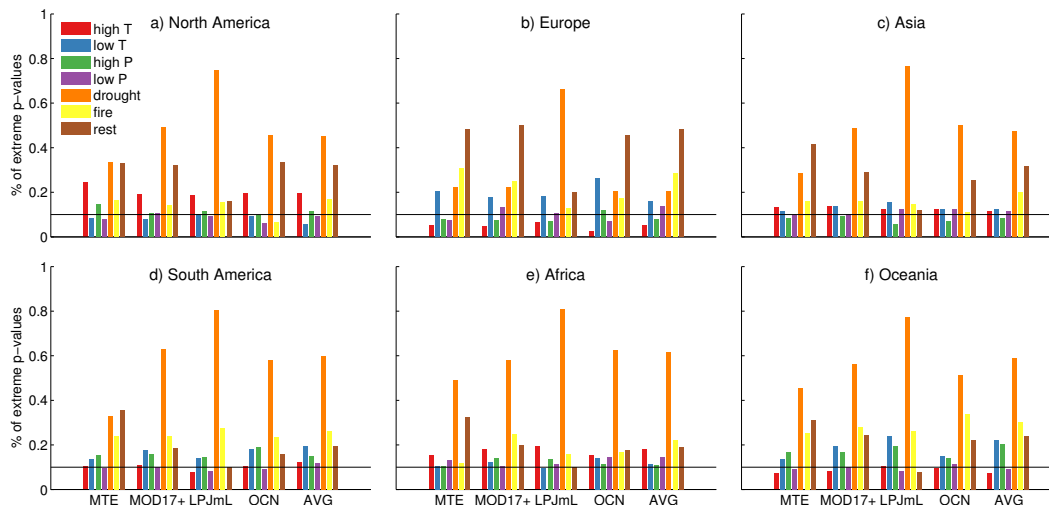


**Fig. 10.** Percentage of extreme  $p$  values ( $p < 0.1$ ) of the 200 largest 1st-percentile GPP extreme events for each of the six continents, all four data sets and the variables high and low temperature ( $T$ , red and blue), high and low precipitation ( $P$ , green and purple), low water availability (drought, orange), and high burned area or fire emissions (fire, yellow). The horizontal line depicts the significance threshold (0.1), i.e. the percentage of events which are expected to have  $p$  values below 0.1 if the data were random. The last bar (rest, brown) depicts the fraction of events that could not be attributed to any of the former variables.

Title Page

Abstract

Introduction

Conclusions

References

Tables

Figures

◀

▶

◀

▶

Back

Close

Full Screen / Esc

Printer-friendly Version

Interactive Discussion



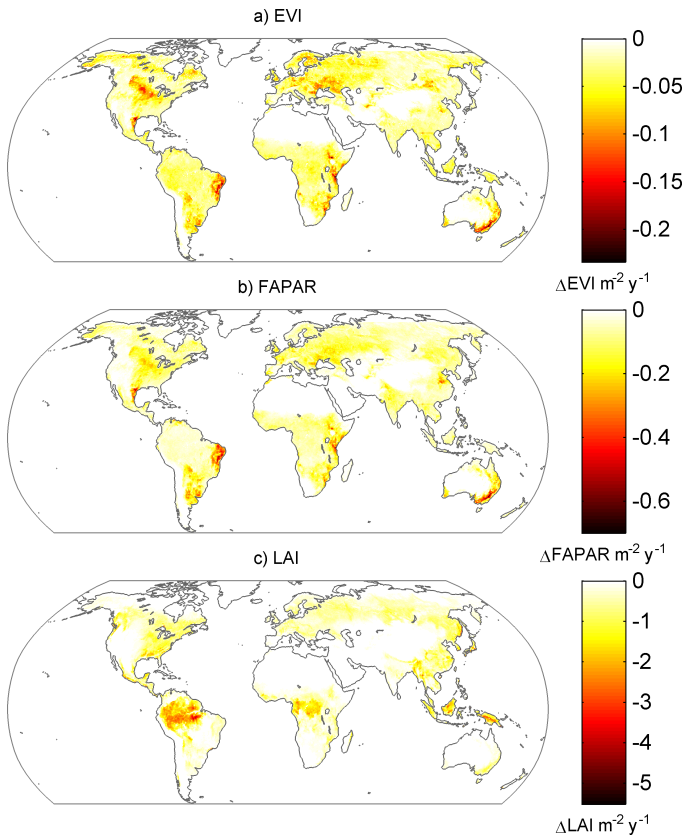


**Fig. 11.** Average impact per year due to negative extreme events in **(a)** EVI (2001–2011), **(b)** FAPAR (1982–2011), and **(c)** LAI (1982–2011). On each continent the 200 largest negative 10th-percentile extremes were computed and merged to obtain a global map. The maps depict the decrease in the respective variable compared to the average year generated by extreme events in that variable.